Nat. Hazards Earth Syst. Sci., 10, 895–899, 2010
www.nat-hazards-earth-syst-sci.net/10/895/2010/

Natural Hazards and Earth System Sciences

Radon concentration in soil gas and radon exhalation rate at the Ravne Fault in NW Slovenia

J. Vaupotič[1], A. Gregorič[1], I. Kobal[1], P. Žvab[2], K. Kozak[3], J. Mazur[3], E. Kochowska[3], and D. Grządziel[3]

[1]Jožef Stefan Institute, Ljubljana, Slovenia
[2]Faculty of Natural Sciences and Engineering, University of Ljubljana, Ljubljana, Slovenia
[3]The Henryk Niewodniczañski Institute of Nuclear Physics, Polish Academy of Science, Kraków, Poland

Received: 30 November 2009 – Revised: 15 March 2010 – Accepted: 10 April 2010 – Published: 23 April 2010

Abstract. The Ravne tectonic fault in north-west (NW) Slovenia is one of the faults in this region, responsible for the elevated seismic activity at the Italian-Slovene border. Five measurement profiles were fixed in the vicinity of the Ravne fault, four of them were perpendicular and one parallel to the fault. At 18 points along these profiles the following measurements have been carried out: radon activity concentration in soil gas, radon exhalation rate from ground, soil permeability and gamma dose rate. The radon measurements were carried out using the AlphaGuard equipment, and GammaTracer was applied for gamma dose rate measurements. The ranges of the obtained results are as follows: 0.9–32.9 kBq m^{-3} for radon concentration (C_{Rn}), 1.1–41.9 mBq m^{-2} s^{-1} for radon exhalation rate (E_{Rn}), 0.5–7.4×10^{-13} m^2 for soil permeability, and 86–138 nSv h^{-1} for gamma dose rate. The concentrations of ^{222}Rn in soil gas were found to be lower than the average for Slovenia. Because the deformation zones differ not only in the direction perpendicular to the fault but also along it, the behaviour of either C_{Rn} or E_{Rn} at different profiles differ markedly. The study is planned to be continued with measurements being carried out at a number of additional points.

1 Introduction

Noble radon gas (^{222}Rn) originates from radioactive transformation of ^{226}Ra in the ^{238}U decay chain in the earth's crust. Only a fraction of the radon atoms so created is able to emanate from the mineral grains and enter the void space, filled either by gas or water. From here, radon moves further by diffusion and, for longer distances, by advection dissolved either in water or in carrier gases. Eventually it exhales into the atmosphere. Radon emanation depends mainly on ^{226}Ra content and mineral grain size, its transport in the earth governed by geophysical and geochemical parameters, while exhalation is controlled by hydrometeorological conditions (Etiope and Martinelli, 2002). Radon activity concentration, measured at the surface, either in a thermal spring or in soil gas is a result of a combined effect of the above mentioned parameters. Among diurnal and seasonal variations which are ascribed to the hydrometeorological parameters, sudden changes (either increase or decrease, also called radon anomalies) may be observed in the time series of radon concentration. These have been found to be related to an increase in seismic (King, 1986; Zmazek et al., 2002) or volcanic (Cigolini et al., 2007; Gasparini and Mantovani, 1978) activity of a region, or activity change of a tectonic or geologic fault (Šebela et al., 2010). On the other hand, radon anomalies in the spatial distribution of radon levels in a region have been observed to coincide with the locations of tectonic and geologic faults, either well expressed on the surface or still hidden (Burton et al., 2004; Swakoñ et al., 2005).

The Ravne fault is one of the faults in NW Slovenia responsible for elevated seismic activity along the Soča (Isonzo) river at the Slovenia-Italy border. In this paper, at various distances from the fault, radon (^{222}Rn) activity concentration in soil gas, radon exhalation rate, soil permeability and gamma dose rate were measured in order to estimate the influence of the fault on radon transport, and thus on the levels of the measured parameters.

Correspondence to: A. Gregorič
(asta.gregoric@ijs.si)

Published by Copernicus Publications on behalf of the European Geosciences Union.

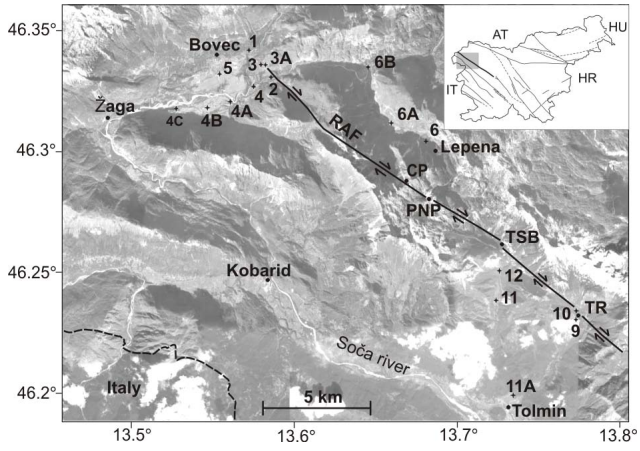

Fig. 1. Location of the Ravne fault with the measurement points indicated. CP – Čez Potoče, PNP – Planina na Polju, RAF – Ravne fault, TR – Tolminske Ravne, TSB – Tolminka Springs basin.

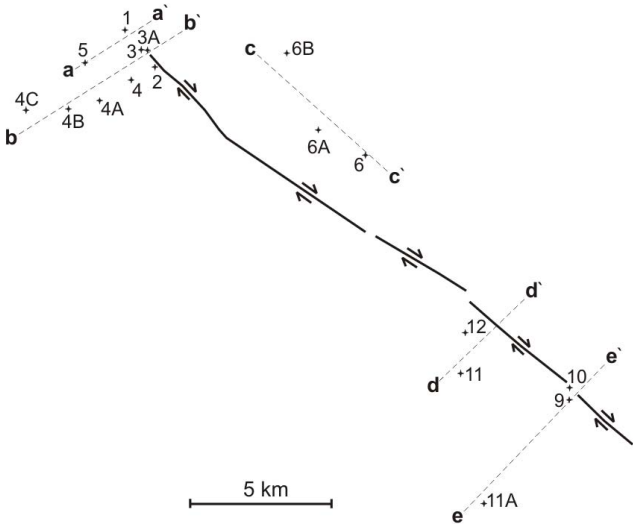

Fig. 2. Measurement profiles.

2 Description of the Ravne Fault

The Ravne Fault is an actively propagating NW-SE trending dextral strike-slip fault in the Julian Alps of NW Slovenia (Fig. 1). Strike-slip displacements on moderate-steep fault planes are responsible for the recent seismic activity that is confined to shallow crustal levels. The fault is growing by interaction of individual right stepping fault segments and breaching of local transtensional step-over zones. The fault geometry is controlled by the original geometry of the NW-SE trending thrust zone, modified by successive faulting within the fault zone. At epicentral depths, the fault system is accommodating recent strain along newly formed fault planes, whereas in upper parts of the crust the activity is distributed over a wider deformation zone that includes reactivated brittle thrust faults. The active deformation along the Ravne fault zone is concentrated in the upper parts of the crust, which is characterized by a high density of older structural elements such as fault planes, fractures and cleavage. The fault is best exposed in its central part around the Tolminka Springs basin over a length of approximately 11 km from the Čez Potoče pass in the NW to the Tolminske Ravne in the SE (Fig. 1) (Kastelic et al., 2008). The Bovec basin, at the north-western end of Ravne fault, is characterised by Triassic and Jurassic carbonates and Cretaceous flysch, covered by fluvio-glacial deposits. The Ravne fault is less exposed to the SE of the Tolminka Springs basin, where it is covered by grass and forested terrain. There are no individual fault planes outcropping between the Tolminka Springs basin and areas SE of Tolminske Ravne. Along that part of the fault trace, the fault exhibits a right-stepping fault segmentation pattern and both segments overstep in the area of Tolminske Ravne.

3 Experimental

3.1 Measurement points

In principle, measurement points were selected on the basis of geology and tectonics of the area. The number of chosen points had to be limited because of mountainous terrain with scarce roads. Some points were not accessible by car, which was necessary to transport equipment. Thus, in total, measurements were performed at 18 points, grouped in five profiles, four perpendicular and one parallel to the fault (Fig. 2).

3.2 Radon in soil gas

The measurement set-up to analyse radon concentration in soil gas C_{Rn} (Bq m^{-3}) consisted of an AlphaGuard PQ 2000 PRO (AG) radon monitor, a soil-gas probe and an Alpha-Pump (AP) (Genitron, Germany) (Fig. 3). Soil gas was pumped through the AG ionization chamber at a flow rate of 0.3 dm^3 min^{-1}. The temporary radon (^{222}Rn) concentrations were registered in one-min intervals over approximately a 20-min period. After initial growth, the concentration became stabilised. The average of the last few stabilised values was taken as the radon concentration in soil gas. At this low flow rate, contribution of thoron (^{220}Rn, half-life 55 s) was negligible (Žunić et al., 2006).

3.3 Radon exhalation from soil

The radon exhalation rate E_{Rn} (Bq m^{-2} s^{-1}) from soil was measured using the Exhalation Box (EB) and the same AG monitor and AP pump as in the previous section (Fig. 4). The air was circulated in the closed circuit for about 90 min and the concentration of radon accumulated in EB was recorded

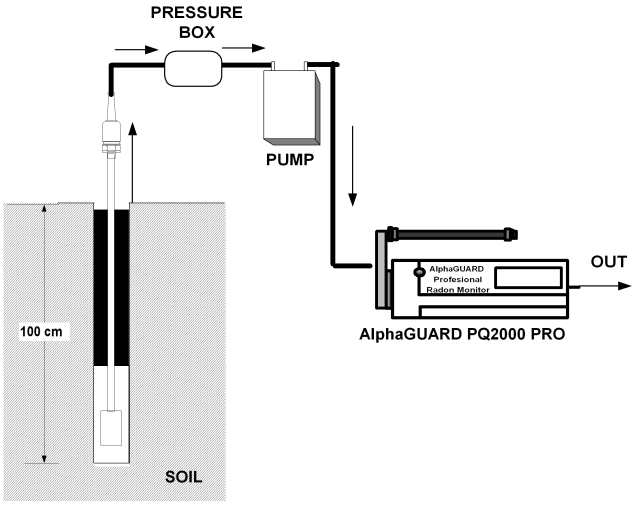

Fig. 3. Soil gas radon measurement.

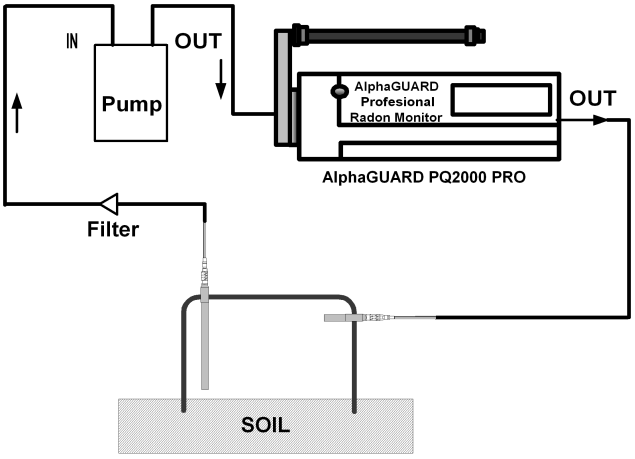

Fig. 4. Radon exhalation measurement.

every 10 min. The exhalation rate was calculated according to the formula:

$$E_{\mathrm{Rn}} = B \cdot \frac{V}{F}$$

where: B – slope of the straight line fixed to the increasing radon concentration points in the EB, V – volume of the EB (m^3), F – surface area covered by EB (m^2) (Žunić et al., 2006).

3.4 Soil permeability

The system to measure soil permeability k_{soil} (m^2) consisted of a Multisensor Unit D/D device (Genitron, Germany) and the same AG monitor, AP pump and soil-gas probe as in Sect. 3.1 (Fig. 5). Soil gas was sucked from soil by soil-gas probe and pumped through the AG and Multisensor. The pressure difference between soil air and open air (ΔP) and flow rate (Q) were measured by the Multisensor D/D. The soil permeability was calculated using a modified equation of Fick's law of diffusion (Janik, 2005):

$$k_{\mathrm{soil}} = \mu \frac{Q}{W \cdot \Delta P}, \quad (1)$$

in which: k_{soil} is soil permeability (m^2), μ is dynamic viscosity of air (Pa s), W is shape parameter of the soil-gas probe (m), Q is soil gas flow rate ($m^3\,min^{-1}$), and ΔP is pressure difference measured (Pa) (Žunić et al., 2006).

3.5 Gamma dose rate

Gamma dose rate $\dot{H}_\gamma$ (nSv h^{-1}) was measured in outdoor air at the height of 1 m above the ground using a GammaTracer TM Wide Type E probe (Genitron, Germany). The values of gamma dose rate were registered in 5-min intervals. The average value of 12–15 records was taken as a final result.

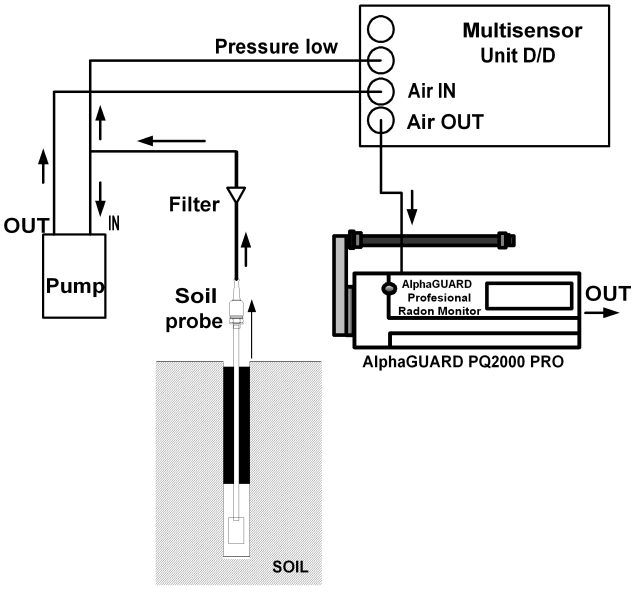

Fig. 5. Soil permeability measurement (Genitron Manual Multisensor D/D).

4 Results and discussion

The results are shown in Table 1. The coordinates and elevations above sea level (a.s.l.) of measurement points together with the dates of measurements are also presented. The measurement points lie from about 350 m to almost 900 m a.s.l. The values of radon concentration in soil gas C_{Rn} were in the range 0.9–22.9 kBq m^{-3} and are lower than the average of 40.1 kBq m^{-3} obtained at 70 points all over Slovenia (Vaupotič, 2009). Also radon exhalation rate E_{Rn} varied substantially from point to point, i.e., from about 1 mBq $m^{-2}\,s^{-1}$ to about 42 mBq $m^{-2}\,s^{-1}$. Soil permeability was found in the range $0.5–7.4\times10^{-13}$ m^2 and may be thus considered as

Table 1. Radon activity concentration in soil gas (C_{Rn}), radon exhalation rate (E_{Rn}), soil permeability (k_{soil}) and gamma dose rate ($\dot{H}_\gamma$) at the Ravne fault.

No	N	E	a.s.l. m	Date in 2008	C_{Rn} kBq m^{-3}	E_{Rn} mBq m^{-2} s^{-1}	k_{soil} m^2	$\dot{H}_\gamma$ nSv h^{-1}
1	20.536	34.414	447	27 Aug	8.4±0.9	15.6±5.0	3.6×10^{-13}	119±6
2	19.853	35.299	894	27 Aug	2.1±0.5	41.9±7.3	3.0×10^{-13}	96±5
3	20.183	34.863	454	27 Aug	16.7±1.2	14.2±4.1	7.4×10^{-13}	110±6
3A	20.155	35.017	459	3 Sep	22.9±3.0	3.0±5.3	7.2×10^{-13}	105±6
4	19.606	34.554	407	27 Aug	9.8±0.7	13.3±4.8	0.5×10^{-13}	104±6
4’	19.646	34.608	400	3 Sep	16.0±2.9	1.1±1.9	4.5×10^{-13}	122±6
4A	19.268	33.756	384	1 Sep	5.0±0.4		3.4×10^{-13}	87±4
4B	19.075	32.907	367	1 Sep	1.8±0.2	8.8±3.5	3.5×10^{-13}	113±6
4C	19.069	31.754	374	1 Sep	4.8±0.5	1.9±2.6	3.5×10^{-13}	114±6
5	19.935	32.290	450	1 Sep	14.8±1.0	40.3±7.1	3.5×10^{-13}	128±6
6	18.249	40.827	648	2 Sep	1.9±0.7	2.2±1.6	4.0×10^{-13}	86±4
6A	18.727	39.577	528	2 Sep	14.7±2.8	15.3±3.3	3.8×10^{-13}	111±6
6B	20.091	38.716	452	3 Sep	2.0±1.0	1.5±1.2	3.7×10^{-13}	86±4
9	13.803	46.292	897	28 Aug	18.9±1.2	9.5±2.9	3.9×10^{-13}	91±5
10	13.998	46.313		28 Aug	8.9±0.8	8.3±3.6	3.8×10^{-13}	87±4
11	14.287	43.385	410	29 Aug	0.9±0.2	7.0±2.3	3.7×10^{-13}	94±5
11A	11.903	44.029	340	29 Aug	9.2±0.7		3.6×10^{-13}	138±7
12	15.027	43.497	509	29 Aug	2.0±0.2	11.7±3.9	6.6×10^{-13}	87±4

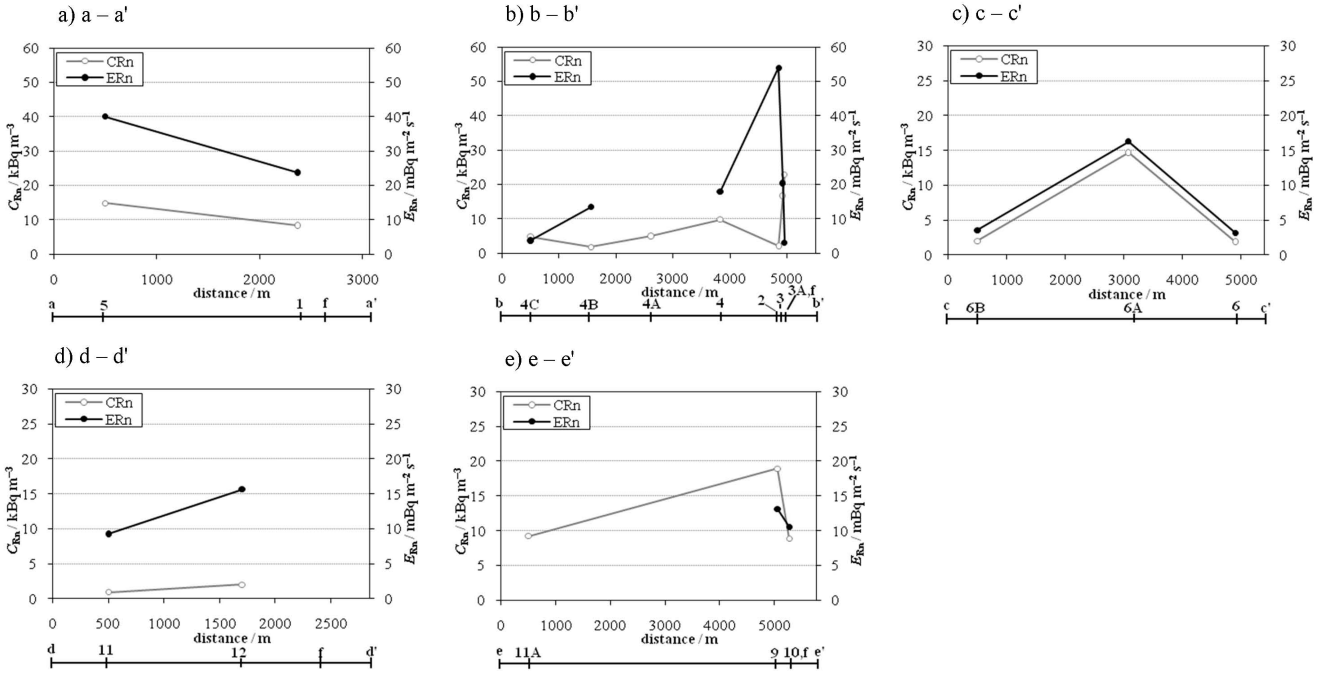

Fig. 6. Radon activity concentrations in soil gas (C_{Rn}) and radon exhalation rate (E_{Rn}) at profile (f – fault): **(a)** a–a’, **(b)** b–b’, **(c)** c–c’, **(d)** d-d’, and **(e)** e–e’.

medium. Gamma dose rate in the range 86–138 nSv h^{-1} is close to the average value obtained for the central part of Slovenia of 118 nSv h^{-1} (Brajnik et al., 1992).

Gas-bearing properties of faults depend on the enhanced permeability of fracture systems. However such permeability is not continuous leading to spotted distribution of soil-gas

anomalies, as shown by Ciotoli et al. (1999). Furthermore, C_{Rn} and E_{Rn} depend also on local characteristics such as thickness of soil covering the underlying deformed rocks. Thus, close to the fault both C_{Rn} and E_{Rn} are lower at the a–a' profile (Fig. 6a) and higher at the d-d' profile (Fig. 6d). The contribution of different stages of rock deformation along the Ravne fault depends locally on the width of the fault deformation zone. Rock fractures could increase radon exhalation from deeper layers and its accumulation in soil (point 5 in the a–a' profile, point 12 in d-d' profile), whereas in the area of intensely deformed rocks, the process of cementation could reduce radon exhalation from deeper layers (point 1 in the a–a' profile and point 10 in the e–e' profile). However deformation zones not only differ in perpendicular direction to the fault but also along its length. Therefore interpretation of radon results is not always possible.

At the b–b' profile (Fig. 6b), where a flat terrain enabled measurements at several distances from the fault, at least on one side of the fault, both C_{Rn} and E_{Rn} appear to be constant in approaching the fault until about 1 km before the fault, where E_{Rn} increases substantially, with a concomitant reduction of C_{Rn} (measurement point 2). The reason for such deviation at measurement point 2 is not understood. At the same time light soil mixed with gravel could also contribute to radon exhalation from the measuring well to the air during the measurement. In close proximity to the fault E_{Rn} is very low, thus enhancing accumulation of radon in soil and consequently increasing C_{Rn}.

The c–c' profile (Fig. 6c) lies along the Lepena valley, parallel to the fault. Higher C_{Rn} and E_{Rn} could be explained by local characteristics of rock deformation and thickness of soil.

5 Conclusions

The results of measurements of radon activity concentration in soil gas, radon exhalation rate from ground, soil permeability and gamma dose rate in the vicinity of Ravne fault in NW Slovenia are presented. The study area was chosen using geological data and the knowledge of fault course.

The concentrations of ^{222}Rn in soil gas were found to be lower than the average for Slovenia. Unlike to the results of similar study (Swakoñ et al., 2005) there was no rapid increase of radon concentration in soil near the fault. Because the deformation zones differ not only in the direction perpendicular to the fault but also along it, the behaviour of either C_{Rn} or E_{Rn} at different profiles differ markedly. Therefore, a full interpretation is very difficult based on the current database. The study is planned to be continued with measurements being carried out at a number of additional points, to build a more complete database to aid interpretation of results. More precise identification of physical characteristics of the ground as well as determination of radium ^{226}Ra in soil profiles would be needed to give a detailed interpretation.

Edited by: T. Przylibski
Reviewed by: two anonymous referees

References

Brajnik, D., Miklavžič, U., and Tomšič, J.: Map of natural radioactivity in Slovenia and its correlation to the emanation of radon, Radiat. Prot. Dosim., 45, 273–276, 1992.

Burton, M., Neri, M., and Condarelli, D.: High spatial resolution radon measurements reveal hidden active faults on Mt. Etna, Geophys. Res. Lett., 31, L07618, doi:10.1029/2003GL019181, 2004.

Cigolini, C., Laiolo, M., and Coppola, D.: Earthquake-volcano interactions detected from radon degassing at Stromboli (Italy), Earth Planet. Sc. Lett., 257, 511–525, 2007.

Ciotoli, G., Etiope, G., Guerra, M., and Lombardi, S.: The detection of concealed faults in the Ofanto Basin using the correlation between soil-gas fracture surveys, Tectonophysics, 301, 321–332, 1999.

Etiope, G. and Martinelli, G.: Migration of carrier and trace gases in the geosphere: an overview, Phys. Earth Planet. In., 129, 185–204, 2002.

Gasparini, P. and Mantovani, M. S. M.: Radon anomalies and volcanic eruptions, J. Volcanol. Geoth. Res., 3, 325–341, 1978.

Janik, M.: Radon transport model and its verification by measurements in houses, IFJ PAN, Krakow, 50–57, 2005.

Kastelic, V., Vrabec, M., Cunningham, D., and Gosar, A.: Neo-Alpine structural evolution and present-day tectonic activity of the eastern Southern Alps: The case of the Ravne Fault, NW Slovenia, J. Struct. Geol., 30, 963–975, 2008.

King, C. Y.: Gas geochemistry applied to earthquake prediction – an overview, J. Geophys. Res.-Solid, 91, 2269–2281, 1986.

Swakoñ, J., Kozak, K., Paszkowski, M., Gradziński, R., Łoskiewicz, J., Mazur, J., Janik, M., Bogacz, J., Horwacik, T., and Olko, P.: Radon concentration in soil gas around local disjunctive tectonic zones in the Krakow area, J. Environ. Radioactiv., 78, 137–149, 2005.

Šebela, S., Vaupotič, J., Koš'ták, B., and Stemberk, J.: Microdisplacements and radon air concentrations in Postojna Cave, Slovenia, J. Cave Karst Stud., in press, 2010.

Vaupotič, J.: Review of radon research in Slovenia, IAEA-TECDOC, 2009.

Zmazek, B., Živčić, M., Vaupotič, J., Bidovec, M., Poljak, M., and Kobal, I.: Soil radon monitoring in the Krško Basin, Slovenia, Appl. Radiat. Isotopes, 56, 649–657, 2002.

Žunić, Z. S., Kobal, I., Vaupotič, J., Kozak, K., Mazur, J., Birovljev, A., Janik, M., Čeliković, I., Ujićć, P., Demajo, A., Krstić, G., Jakupi, B., Quarto, M., and Bochicchio, F.: High natural radiation exposure in radon spa areas: a detailed field investigation in Niška Banja (Balkan region), J. Environ. Radioactiv., 89, 249–260, 2006.